Copy 1

ARR No. L5H11

NATIONAL ADVISORY COMMITTEE FOR AERONAUTICS

WARTIME REPORT

ORIGINALLY ISSUED
October 1945 as
Advance Restricted Report L5H11

COMPARISON BETWEEN CALCULATED AND MEASURED LOADS ON WING AND HORIZONTAL TAIL IN PULL-UP MANEUVERS

By Cloyce E. Matheny

Langley Memorial Aeronautical Laboratory
Langley Field, Va.

NACA

WASHINGTON

NATIONAL ADVISORY COMMITTEE FOR AERONAUTICS

ADVANCE RESTRICTED REPORT

COMPARISON BETWEEN CALCULATED AND MEASURED LOADS ON WING AND HORIZONTAL TAIL IN PULL-UP MANEUVERS

By Cloyce E. Matheny

SUMMARY

Comparisons have been made of measured and calculated loads on the wing and the horizontal tail in pull-up maneuvers for six airplanes ranging in weight from 4,700 to 48,000 pounds. The calculated loads were based on the control motions measured in flight. The aerodynamic characteristics of the airplanes required for the calculations were either obtained directly from wind-tunnel data or computed.

Good agreement was obtained between calculated and measured loads for a specified elevator deflection when reliable wind-tunnel data were available and when the airplane maneuvers were consistent with the assumptions. The fact that only fair agreement was obtained in some of the cases was attributed either to poor quantitative knowledge of the aerodynamic parameters or to the violation of the assumptions on which the method is based.

INTRODUCTION

During the past few years much work has been done in an attempt to relate tail loads more closely to the aerodynamic and geometric characteristics as well as to the functional requirements of the airplane. In various reports that have been written on this subject either of two approaches has been used; namely, (1) to proceed from a specified control motion to the determination of the wing and tail loads, as in reference 1; or (2) to proceed from a specified wing-load variation to the determination of the tail load and elevator motions, as in reference 2. Both methods depend on a solution of the equations of motion for a rigid body and consequently require a knowledge of the aerodynamic and geometric characteristics of the airplane. The loads computed are the resultant air loads that act over the horizontal surfaces; therefore the solutions obtained do not indicate possible adverse chordwise or spanwise distributions or the buffeting tail-load increment.

Recently a method based on the determination of the wing and tail loads for a specified control motion has been recommended as a part of the airplane load design requirements for the Army (references 3 and 4). Since the application of this method requires considerable time, it seems desirable to determine the agreement that can be expected between measured and calculated results.

The object of the present report is to give results of comparisons between measured and calculated wing and tail loads in pull-up maneuvers for six airplanes ranging in weight from 4,700 to 48,000 pounds. The flight data presented herein are typical and are taken from unpublished results measured in flight during the past five years.

SYMBOLS

W airplane weight, pounds

g acceleration of gravity, feet per second^2

m airplane mass, slugs (W/g)

S gross wing area including area within fuselage, square feet

S_t gross horizontal-tail area including area intercepted by fuselage, square feet

b wing span, feet

b_t tail span, feet

k_Y radius of gyration about pitching axis, feet

I_Y moment of inertia about pitching axis, slug-feet^2

x_t length from center of gravity of airplane to aerodynamic center of tail (negative for conventional airplanes), feet

σ	air density ratio (ρ/ρ_o)
V	airspeed, feet per second
V_e	equivalent airspeed, miles per hour $\left(\frac{V}{1.467}\sigma^{1/2}\right)$
M	Mach number
ρ	mass density of air, slugs per cubic foot
q	dynamic pressure, pounds per square foot $\left(\frac{1}{2}\rho V^2\right)$
η	tail efficiency factor $\left(q_t/q\right)$
L	lift, pounds
C_L	lift coefficient (L/qS)
C_m	pitching-moment coefficient of airplane without horizontal tail $\left(\text{Moment} \times \frac{b}{qS^2}\right)$
α	wing angle of attack, radians
α_t	equivalent tail angle of attack, radians
δ	elevator angle, radians
ϵ	downwash angle at tail, radians $\left(\frac{d\epsilon}{d\alpha}\alpha\right)$
K	empirical constant denoting ratio of damping moment of complete airplane to damping moment of tail alone
n	airplane load factor
K_1', K_2', K_3'	nondimensional constants occurring in basic differential equation

The notations $\dot{\alpha}$ and $\ddot{\alpha}$ denote single and double differentiations with respect to time.

Subscripts:

t tail

0 sea-level conditions

METHOD

Although, as previously stated, there are a number of methods available for computing the wing and tail loads for any elevator motion, the method used herein for all the computations is that described in reference 1. This method is similar, as far as basic assumptions are concerned, to that of reference 4 but differs in small details such as type of axes used and computational procedures employed. The basic assumptions underlying the method are that:

(1) The change in load factor in a pull-up or pull-out, as a result of attitude change, is small with respect to that due to change in angle of attack

(2) The aerodynamic quantities are linear functions of angle of attack

(3) The speed is constant during the maneuver

(4) The effects of flexibility are neglected

With these assumptions the differential equation of motion for a unit elevator deflection becomes

$$\ddot{\alpha} + K_1'\dot{\alpha} + K_2'\,\Delta\alpha = K_3'\,\Delta\delta(1) \qquad (1)$$

where K_1', K_2', and K_3' are functions of the aerodynamic and geometric characteristics. With the unit solution of equation (1) known, $\Delta\alpha$ and $\dot{\alpha}$ are evaluated for any control motion by applying Duhamel's integral theorem. The increment in load factor Δn is related to $\Delta\alpha$ through the equation

$$\Delta n = \frac{dC_L}{d\alpha}\frac{\Delta\alpha\,q}{W/S} \qquad (2)$$

The increment in equivalent tail angle of attack is related to $\Delta\alpha$ and $\dot{\alpha}$ through the equation

$$\Delta\alpha_t = \Delta\alpha\left(1 - \frac{d\epsilon}{d\alpha} - \frac{dC_L}{d\alpha}\frac{\rho}{2}\frac{S}{m}\frac{x_t}{\sqrt{\eta}}\right) - \dot{\alpha}\frac{x_t}{V}\left(\frac{d\epsilon}{d\alpha} + \frac{1}{\sqrt{\eta}}\right) + \frac{d\alpha_t}{d\delta}\Delta\delta \qquad (3)$$

and finally the tail load follows from equation (3) as

$$\Delta L_t = \frac{dC_{L_t}}{d\alpha_t}\Delta\alpha_t\,\eta q S_t \qquad (4)$$

BASIC DATA FOR CALCULATIONS

Flight data.- The flight data used in the calculations are given in figure 1. This figure shows the time variation of airspeed and elevator position measured during either pull-ups or dive pull-outs made with the SB2C-1, PBM-3, P-40K, XP-51, BT-9B, and B-24D airplanes. The wing and tail loads corresponding to these control motions and airspeeds are included in the figures giving the comparisons between calculated and measured values.

Aerodynamic parameters.- The aerodynamic parameters required are:

$\frac{dC_L}{d\alpha}$ slope of airplane lift curve. This quantity was obtained, whenever possible, from wind-tunnel tests of either the complete airplane or a model. For the PBM-3 seaplane, $\frac{dC_L}{d\alpha}$ was estimated from tests of a model of a similar seaplane.

$\frac{dC_{L_t}}{d\alpha_t}$ slope of tail-plane lift curve. This quantity was obtained, whenever possible, from wind-tunnel tests of the isolated tail or from tail-on tests made with different stabilizer settings. When such data were not available from tunnel tests, they were obtained from reference 5.

$\frac{d\epsilon}{d\alpha}$ rate of change of downwash at tail with angle of attack. This factor was determined, whenever possible, from results of downwash surveys behind a particular model or from moment differences between tail-on and tail-off wind-tunnel tests. When experimental results were not available, this factor was computed from the results given in reference 6.

η tail efficiency factor. When possible, this factor was obtained from total-head surveys in the region of the tail. When such surveys were not available, the method suggested in reference 1 was used to determine this quantity.

K empirical damping factor, ratio of damping moment of complete airplane to that of tail. In the calculations this value was taken either as 1.1 or 1.25, depending upon the airplane configuration.

$\frac{dC_{L_t}}{d\delta}$ elevator effectiveness. This quantity was obtained from reference 5 whenever specific wind-tunnel tests were not available for its determination.

$\frac{dC_m}{d\alpha}$ slope of airplane moment-coefficient curve (minus tail). This quantity was determined from wind-tunnel tests of either a model or the airplane. The values obtained from the tunnel were adjusted for the particular center-of-gravity position of the flight tests. For the PBM-3 seaplane, $\frac{dC_m}{d\alpha}$ was estimated from tests of a model of a similar seaplane.

$\frac{dC_{m_t}}{d\delta}$ rate of change of tail moment coefficient with elevator deflection for isolated tail. Except in the case of the BT-9B airplane, this quantity was computed from results similar to those given in reference 7.

The aerodynamic parameters for all airplanes under consideration are compiled in table I. Low-speed wind-tunnel data were used in all the foregoing parameters except for a few values on the XP-51 airplane, which were taken from wind-tunnel data at the flight Mach number. The remainder of the parameters for this airplane were corrected for the effects of Mach number by the Prandtl-Glauert factor $\frac{1}{\sqrt{1 - M^2}}$. No corrections were made to the low-speed values for the other airplanes.

In order to check the validity of these calculations, an individual case was calculated whereby the effects of compressibility were taken into account for a dive by the SB2C-1 airplane at a Mach number of 0.61. Results from these calculations showed that at this Mach number the loads calculated using parameters corrected for compressibility effects were not appreciably different from the loads calculated using low-speed values of the parameters.

<u>Physical and geometric characteristics</u>.- The physical and geometric characteristics of the airplanes were determined principally from manufacturers' data and are presented in detail in table II.

RESULTS

The increments in acceleration and tail loads computed from the basic data given in figure 1 and in tables I and II are shown in figures 2 to 10. In these figures the dashed lines represent the calculated values and the full lines, the measured values. The measured tail loads were obtained by use of pressure distributions, electrical strain gages, beam deflections, or dynamometers. Table III summarizes the tail load conditions represented in the various figures and gives the estimated accuracy of the measurements.

In these comparisons (figs. 2 to 10) the tail loads given as "measured tail loads" have been converted to air loads; that is, inertia effects have been eliminated when necessary. In each case the comparison is made of the increments in load measured with respect to the loads at the instant the maneuver was considered to have been started.

The measured accelerations were obtained with a standard NACA accelerometer located near the center of gravity. The measured accelerations are accurate to about ±0.05g.

DISCUSSION

The comparisons given in figures 2 to 4 for the SB2C-1 airplane indicate good agreement between the calculated and measured tail loads for the three typical dive pull-outs chosen. The measured data were obtained at Mach numbers below the critical value for this airplane, 0.67, and in relatively quick pull-ups. Such conditions favor the assumptions on which the calculations were based: namely, linear variation of aerodynamic quantities with angle of attack, and small attitude and speed changes during the maneuver. A great deal of consistent wind-tunnel data were also available for this airplane in the form of force tests and wake surveys behind a model. Although the flight conditions shown in figures 2 to 4 are not the critical ones for which calculations would ordinarily be made, the fact that the calculated and measured tail loads per g are approximately the same indicates that the method could be used to predict loads with good accuracy for conditions other than those tested.

The comparison shown in figure 5 for a pull-up with the PBM-3 seaplane shows good agreement in the acceleration increments obtained. This calculation represents one for which a minimum of wind-tunnel data was available. The pull-up was made from a shallow dive and in such a way that both small attitude and velocity change resulted. Although no tail loads were measured in flight on this seaplane, the calculated tail loads are thought to be of interest.

The results shown in figure 6 for a dive pull-out with the P-40K airplane show poor agreement between the acceleration and tail-load increments. The disagreement can be attributed only to a lack of quantitative knowledge of the aerodynamic parameters rather than to any large departures from the assumptions on which the methods are based. The aerodynamic parameters believed to be principally at fault in the P-40K results are $dC_m/d\alpha$ and and $d\epsilon/d\alpha$. In the determination of these quantities, data were available from low-speed tests made at the Air Technical Service Command, Wright Field on a small propellerless model of an early version of the P-40 series.

In addition, some tests were available from the Langley full-scale tunnel of the XP-40 and P-40K airplanes. Data from the Langley tests were somewhat limited since the tests were conducted for other purposes. The data that could be pieced together from these sources indicated not only a large value of $d\epsilon/d\alpha$ but also considerable scatter.

In the light of the results given in figure 6, it may be stated that a smaller value of either $dC_m/d\alpha$ or $d\epsilon/d\alpha$ would have resulted in a closer agreement as regards the maximum loads at the expense of a poorer agreement in the loads sequence. This reasoning is based on experiences with computations of this nature (see reference 8) and on the fact that the differential equation of motion on which the calculations are based corresponds to that of a forced vibration with viscous damping. For such a system relatively large changes in damping would produce only slight changes in the frequency; whereas changes in the factors influencing the restoring force - that is, $d\epsilon/d\alpha$ and $dC_m/d\alpha$ - would change the frequency. Closer agreement would result in this particular case if either or both $dC_m/d\alpha$ and $d\epsilon/d\alpha$ should be decreased simultaneously with an increase in the damping factor K and/or the radius of gyration k_Y. The increase that would be required in these factors to obtain a close agreement would have to be larger than could be attributed to possible inaccuracies in these quantities.

In figure 7, for the XP-51 airplane, poor agreement was obtained between measured and calculated wing loads in spite of the fact that extensive wind-tunnel data were available for this airplane; whereas in figure 8 closer agreement was obtained. Figure 1(a) shows that large speed changes occurred with the pull-out shown in figure 7, and the corresponding attitude changes were probably large. Figure 8 indicates that better agreement in acceleration increments was obtained in a relatively short-period pull-out than in the pull-out represented by figure 7, which required 16 seconds. The experimental accuracy of tail-load measurement was relatively poorer than for the SB2C-1 and P-40K airplanes (figs. 2 to 4 and 6).

The agreement shown in figure 9 for the BT-9B airplane is only fairly close in spite of the fact that complete aerodynamic data were available for the actual airplane and tail surfaces from tests made in the Langley full-scale tunnel. All the flight tests available from which a pull-up could be chosen, however, were of such a nature that large changes in both speed and attitude occurred during the maneuver and on this account poor agreement might be expected. Also the flight tests were conducted at a center-of-gravity location and speed such that the measured tail loads were relatively small.

Figure 10 shows the comparison between calculated and measured increments of acceleration and tail load for the B-24D airplane. No conclusions can be drawn concerning the lack of agreement in the curves for tail-load increment because of the sparse strain-gage installation used in obtaining the tail loads. In the interpretation of the flight results to obtain tail loads, it was necessary to estimate both chordwise and spanwise load centers. Errors in the estimation of these centers would cause errors in tail load in individual runs that are even larger than those previously listed.

CONCLUSIONS

Comparisons have been made of measured and calculated loads on the wing and the horizontal tail in pull-up maneuvers for six airplanes ranging in weight from 4,700 to 48,000 pounds.

1. The agreement between calculated and measured wing- and tail-load increments for a specified elevator deflection was good when reliable wind-tunnel data were available and when the airplane maneuvers were in accord with the assumptions.

2. Poor agreement was obtained for several comparisons. The poor agreement could be traced either to poor quantitative knowledge of the aerodynamic parameters or to the violations of the assumptions on which the method is based.

Langley Memorial Aeronautical Laboratory
National Advisory Committee for Aeronautics
Langley Field, Va.

REFERENCES

1. Pearson, Henry A.: Derivation of Charts for Determining the Horizontal Tail Load Variation with Any Elevator Motion. NACA ARR, Jan. 1943.

2. Dickinson, H. B.: Maneuverability and Control Surface Strength Criteria for Large Airplanes. Jour. Aero. Sci., vol. 7, no. 11, Sept. 1940, pp. 469-477.

3. Perkins, Courtland D., and Lees, Lester: Maneuver Loads on Horizontal Tail Surfaces of Airplanes. AAF TR No. 4852, Materiel Div., Army Air Forces, Nov. 19, 1942.

4. Perkins, Courtland D.: Non-Dimensional Chart Method for Computing the Maneuver Loads on the Horizontal Tail Surfaces of Airplanes. AAF TR No. 4925, Materiel Command, Army Air Forces, May 13, 1943.

5. Silverstein, Abe, and Katzoff, S.: Aerodynamic Characteristics of Horizontal Tail Surfaces. NACA Rep. No. 688, 1940.

6. Silverstein, Abe, and Katzoff, S.: Design Charts for Predicting Downwash Angles and Wake Characteristics behind Plain and Flapped Wings. NACA Rep. No. 648, 1939.

7. Street, William G., and Ames, Milton B., Jr.: Pressure-Distribution Investigation of an N.A.C.A. 0009 Airfoil with a 50-Percent-Chord Plain Flap and Three Tabs. NACA TN No. 734, 1939.

8. Pearson, H. A., and Garvin, J. B.: An Analytical Study of Wing and Tail Loads Associated with an Elevator Deflection. NACA ARR, June 1941.

TABLE I.- AERODYNAMIC PARAMETERS FOR AIRPLANES UNDER CONSIDERATION

Parameter \ Airplane	SB2C-1			PBM-3	P-40K	XP-51		BT-9B	B-24D
	Dive 6	Dive 10	Dive 11			Flight 26	Flight 10		
Slope of airplane lift curve, $\frac{dC_L}{d\alpha}$, radians	[a]4.50	[a]4.50	[a]4.50	[i]5.00	[a]5.16	[a]6.05	[a]5.38	[h]4.67	[a]5.30
Slope of tail-plane lift curve, $\frac{dC_{L_t}}{d\alpha_t}$, radians	[b]2.98	[b]2.98	[b]2.98	[b]4.30	[b]3.04	[b,m]3.50	[b,m]3.44	[j]2.83	[b]4.33
Downwash factor, $\frac{d\epsilon}{d\alpha}$	[d]0.54	[d]0.54	[d]0.54	[c]0.53	[k]0.70	[e]0.46	[e]0.56	[e]0.42	[e]0.32
Tail efficiency factor, η	[d]1.00	[d]1.00	[d]1.00	[g]1.00	[l]1.02	[e]0.99	[e]0.83	[e]0.81	[e,d]0.90
Empirical damping factor, K	[g]1.1	[g]1.1	[g]1.1	[g]1.1	[g]1.1	[g]1.1	[g]1.1	[g]1.25	[g]1.25
Elevator effectiveness, $\frac{dC_{L_t}}{d\delta}$, radians	[b]1.49	[b]1.49	[b]1.49	[b]1.83	[b]1.85	[b,m]1.86	[b,m]1.82	[j]1.56	[b]2.30
Slope of airplane moment curve (minus tail), $\frac{dC_m}{d\alpha}$, radian	[a]0.480	[a]0.456	[a]0.468	[i]0.400	[g]0.446	[a]0.567	[a]0.289	[h]0.176	[a]0.[illegible]56
Tail moment change with elevator angle, $\frac{dC_{m_t}}{d\delta}$, radian	[f]0.55	[f]0.55	[f]0.55	[f]0.50	[f]0.50	[f,m]0.50	[f,m]0.50	[j]0.59	[f]0.44
V_e, airspeed, mph $\left(V_e = \frac{V}{1.467}\sigma^{1/2}\right)$	320	400	324	190	384	410	316	146	250
Pressure altitude, h, ft	6,210	8,100	6,660	5,800	6,000	16,600	19,400	6,000	9,500
Air mass density, ρ, slug/ft^3	0.001974	0.001860	0.001950	0.002000	0.001988	0.001419	0.001259	0.001988	0.001780

[a]From wind-tunnel tests of model.
[b]Reference 5.
[c]Reference 6.
[d]Survey behind model without tail plane.
[e]Derived from wind-tunnel tests by moment differences as in reference 1.
[f]From tests of isolated airfoils with various flap-chord ratios.
[g]Assigned.
[h]From wind-tunnel tests of airplane.
[i]Obtained by comparison with results of similar model.
[j]From wind-tunnel tests of actual tail plane.
[k]Averaged from flight and wind-tunnel tests.
[l]Survey taken on actual airplane with tail in place.
[m]Corrected for compressibility by factor $\frac{1}{\sqrt{1 - M^2}}$.

NATIONAL ADVISORY
COMMITTEE FOR AERONAUTICS

TABLE II. - PHYSICAL AND GEOMETRIC CHARACTERISTICS FOR AIRPLANES UNDER CONSIDERATION

Characteristics \ Airplane	SB2C-1			PBM-3	P-40K	XP-51		BT-9B	B-24D
	Dive 6	Dive 10	Dive 11			Flight 26	Flight 10		
Gross wing area, S, sq ft	423	423	423	1407	236	233.2	233.2	248	1048
Gross horizontal-tail area, S_t, sq ft	107.4	107.4	107.4	242	48.6	41.96	41.96	49	198
Airplane weight, W, lb	11,983	11,755	11,910	45,000	8,140	7,780	7,575	4,667	48,000
Wing span, b, ft	50	50	50	118	37.29	37.03	37.03	42	110
Horizontal-tail span, b_t, ft	19.04	19.04	19.04	28	12.8	13.18	13.18	13	26
Radius of gyration of airplane, k_Y, ft	6.5	6.5	6.5	15.0	5.9	5.4	5.4	5.9	10.5
Tail length, x_t, ft	-17.7	-17.7	-17.7	-41.0	-16.15	-15.75	-15.95	-15.24	-33.4
Moment of inertia of airplane, I_Y, slug-ft^2	15,690	15,420	15,620	314,200	8,790	7,057	6,870	4,987	163,750
Center of gravity of airplane, percent M.A.C.	27.5	26.9	27.2	28.0	30.6	29.0	26.3	21.3	29.0

NATIONAL ADVISORY
COMMITTEE FOR AERONAUTICS

TABLE III.- SUMMARY OF TAIL LOAD CONDITIONS

Fig.	Airplane	Maneuver	Method of measurement	Estimated accuracy (lb)
2 3 4	SB2C-1	Dive pull-out	Pressure distribution	±50
5	PBM-3	Pull-up	Tail loads not measured	---------
6	P-40K	Dive pull-out	Pressure distribution	±50
7 8	XP-51	Gradual dive pull-out Dive pull-out	Beam deflection	±150
9	BT-9B	Pull-up	Calibrated springs inserted between tail and fuselage	±50
10	B-24D	Dive pull-out	Strain gages	±300

NATIONAL ADVISORY
COMMITTEE FOR AERONAUTICS

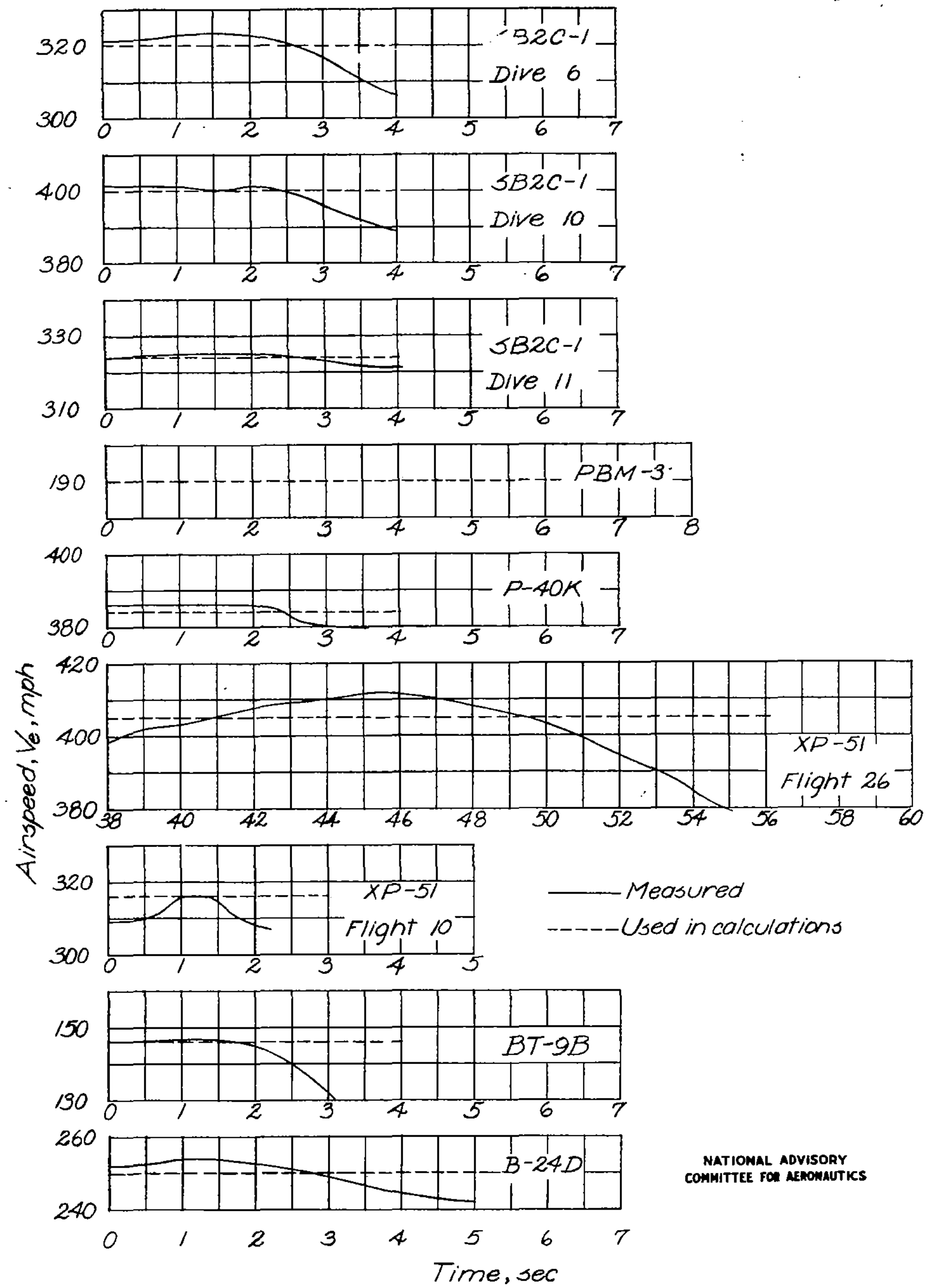

(a) Airspeed time histories.

Figure 1.- Basic flight data for all airplanes under consideration. $V_e = \frac{V}{1.467}\sigma^{\frac{1}{2}}$.

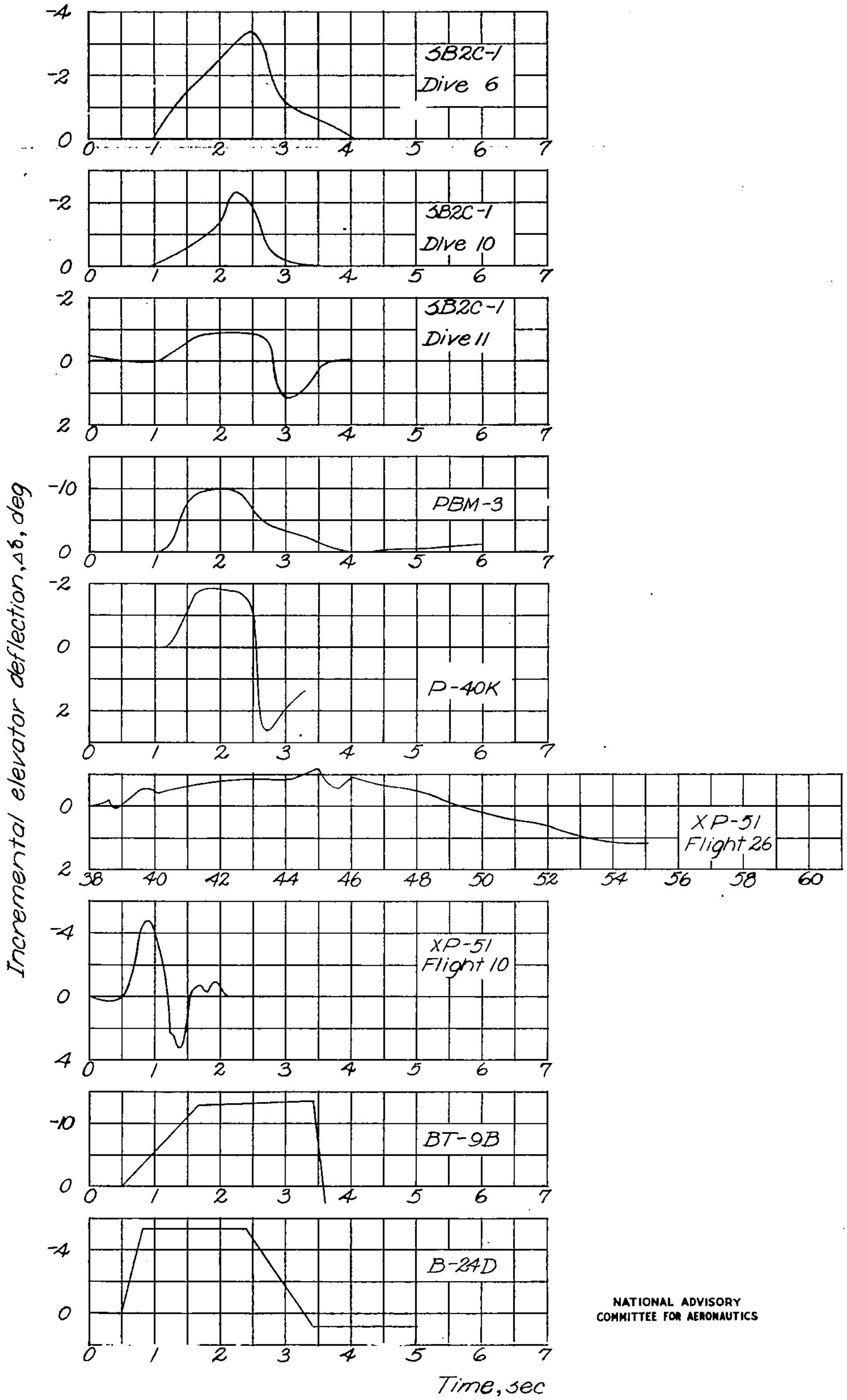

(b) Incremental-elevator-deflection time histories.

Figure 1.- Concluded.

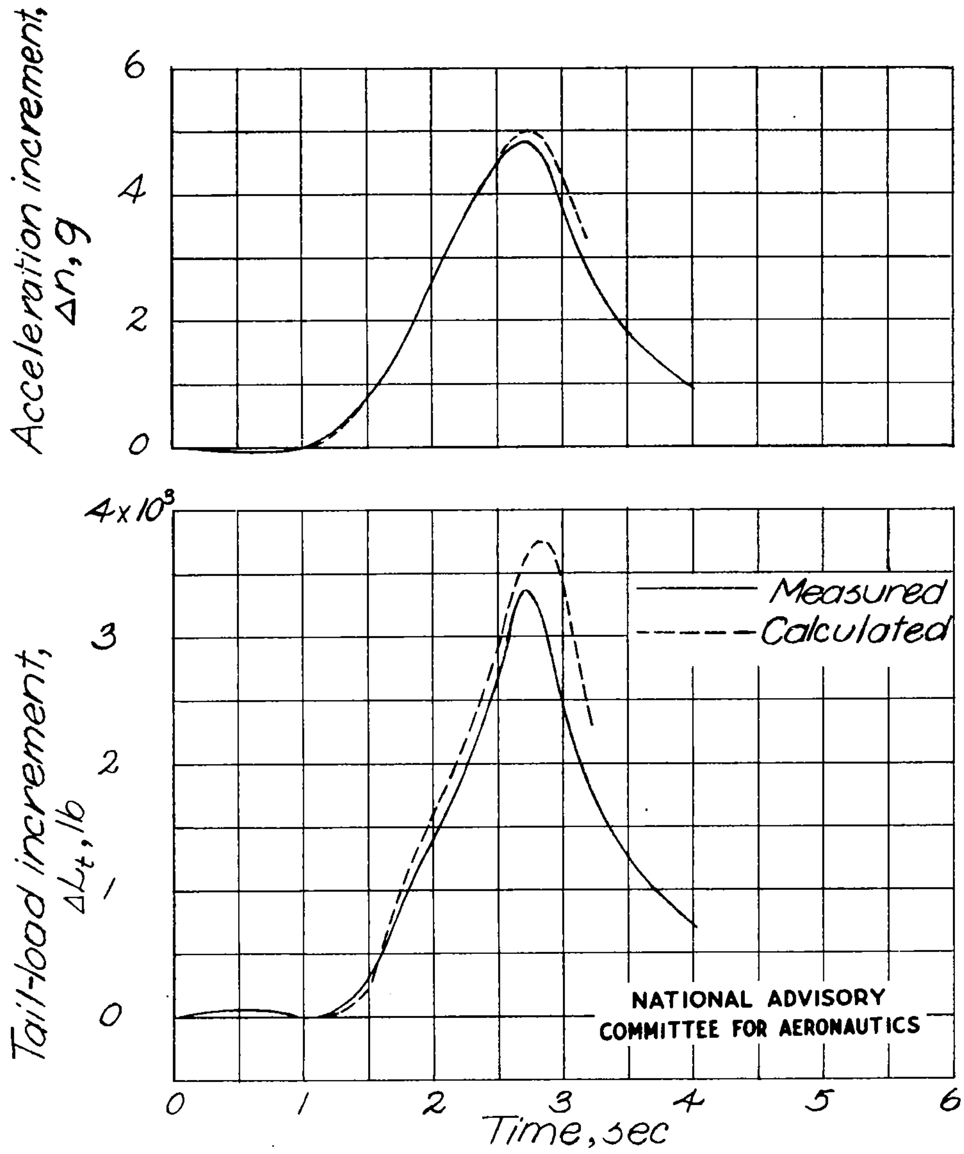

Figure 2.- Comparison between measured and calculated tail-load and acceleration increments during a dive pull-out in an SB2C-1 airplane. Dive 6.

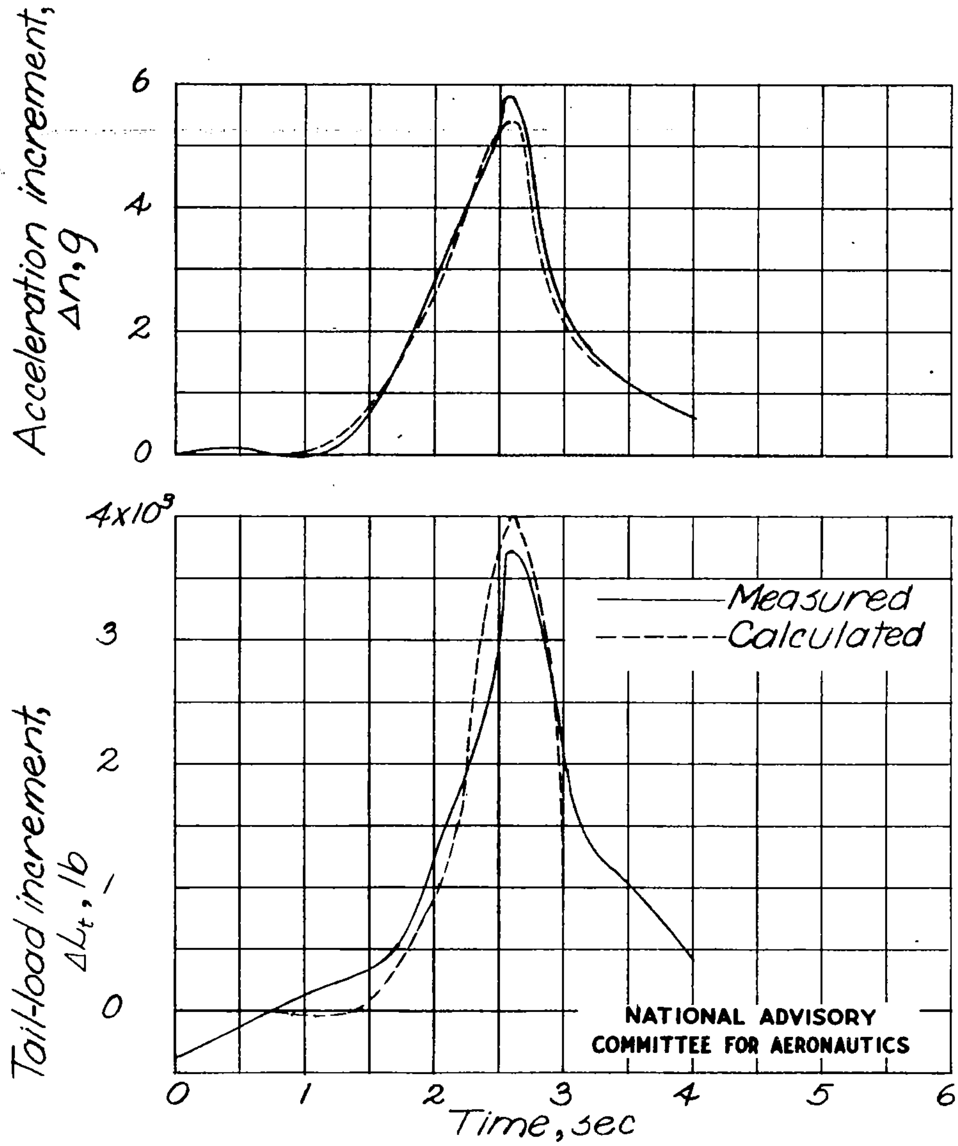

Figure 3.- Comparison between measured and calculated tail-load and acceleration increments during a dive pull-out in an SB2C-1 airplane. Dive 10.

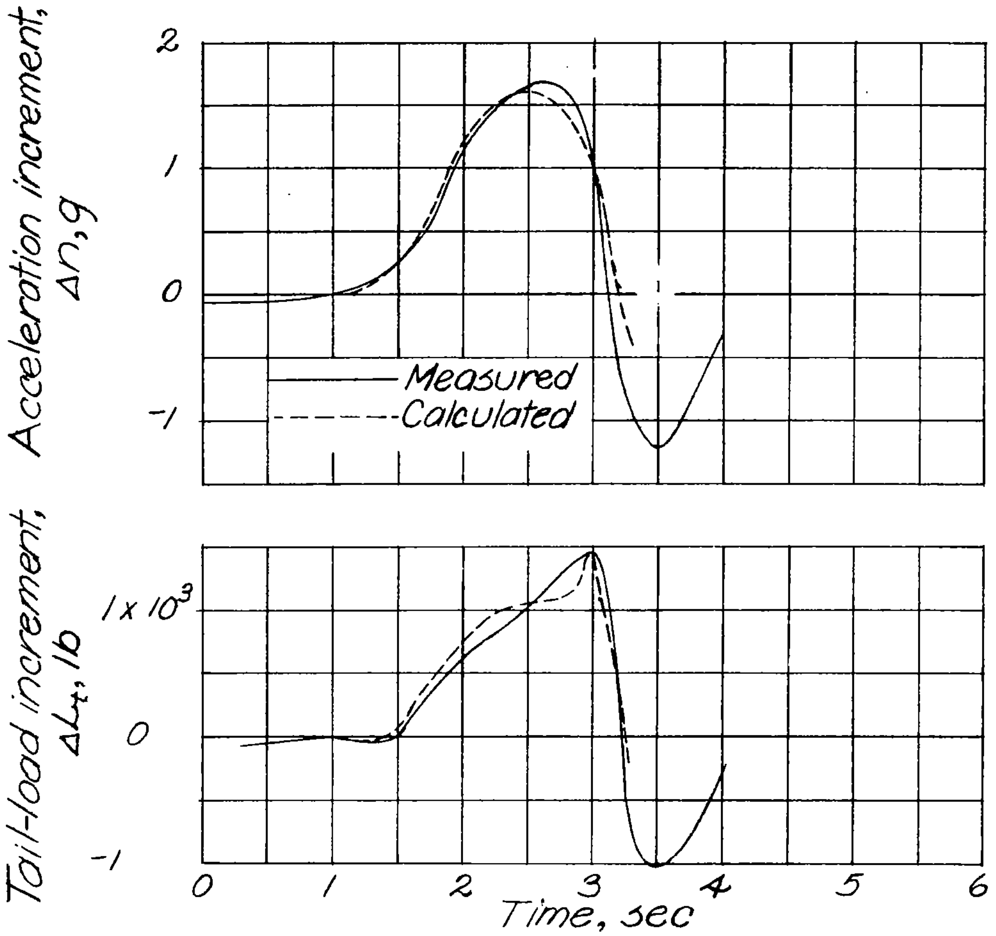

Figure 4.- Comparison between measured and calculated tail-load and acceleration increments during a dive pull-out in an SB2C-1 airplane. Dive 11.

NATIONAL ADVISORY COMMITTEE FOR AERONAUTICS

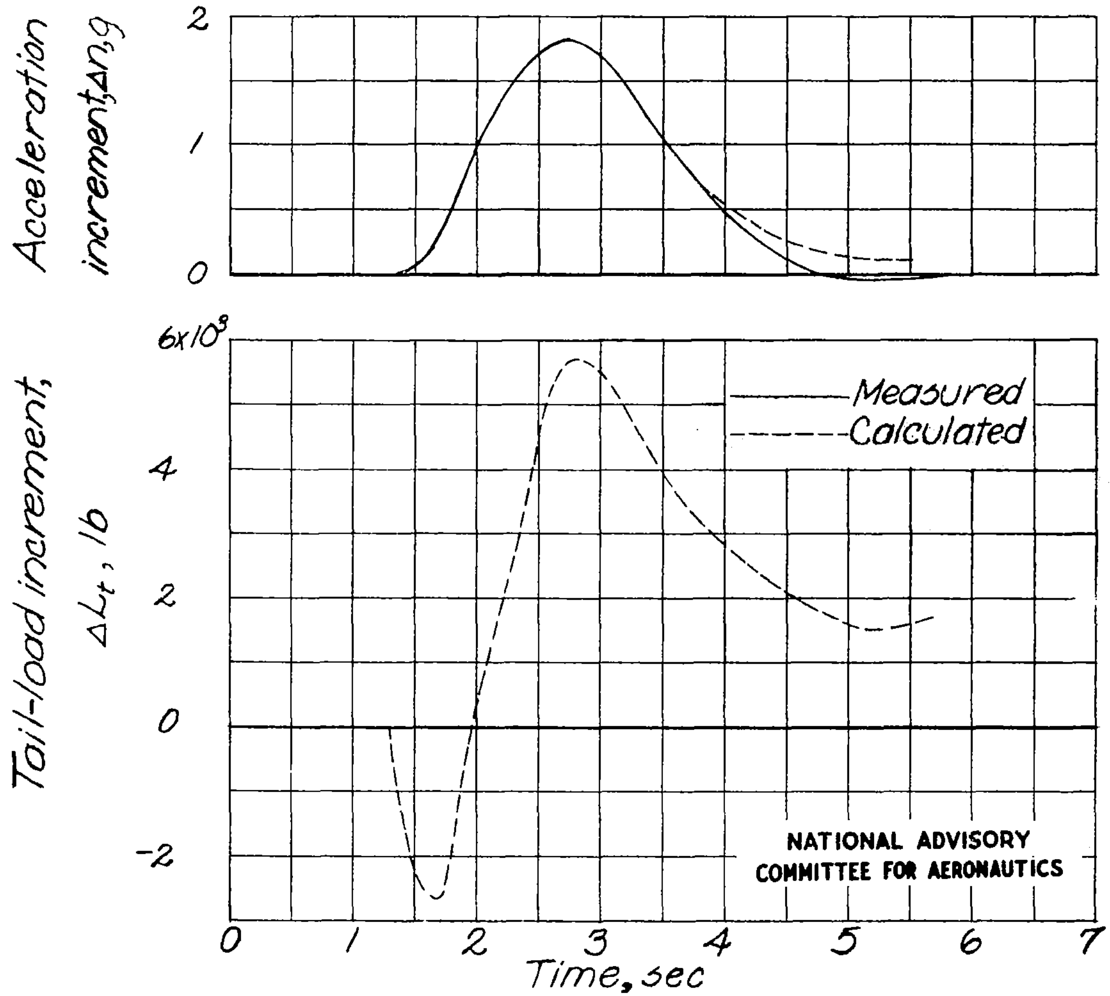

Figure 5.- Comparison between measured and calculated acceleration increments during a pull-up in a PBM-3 airplane. (No tail load measured.)

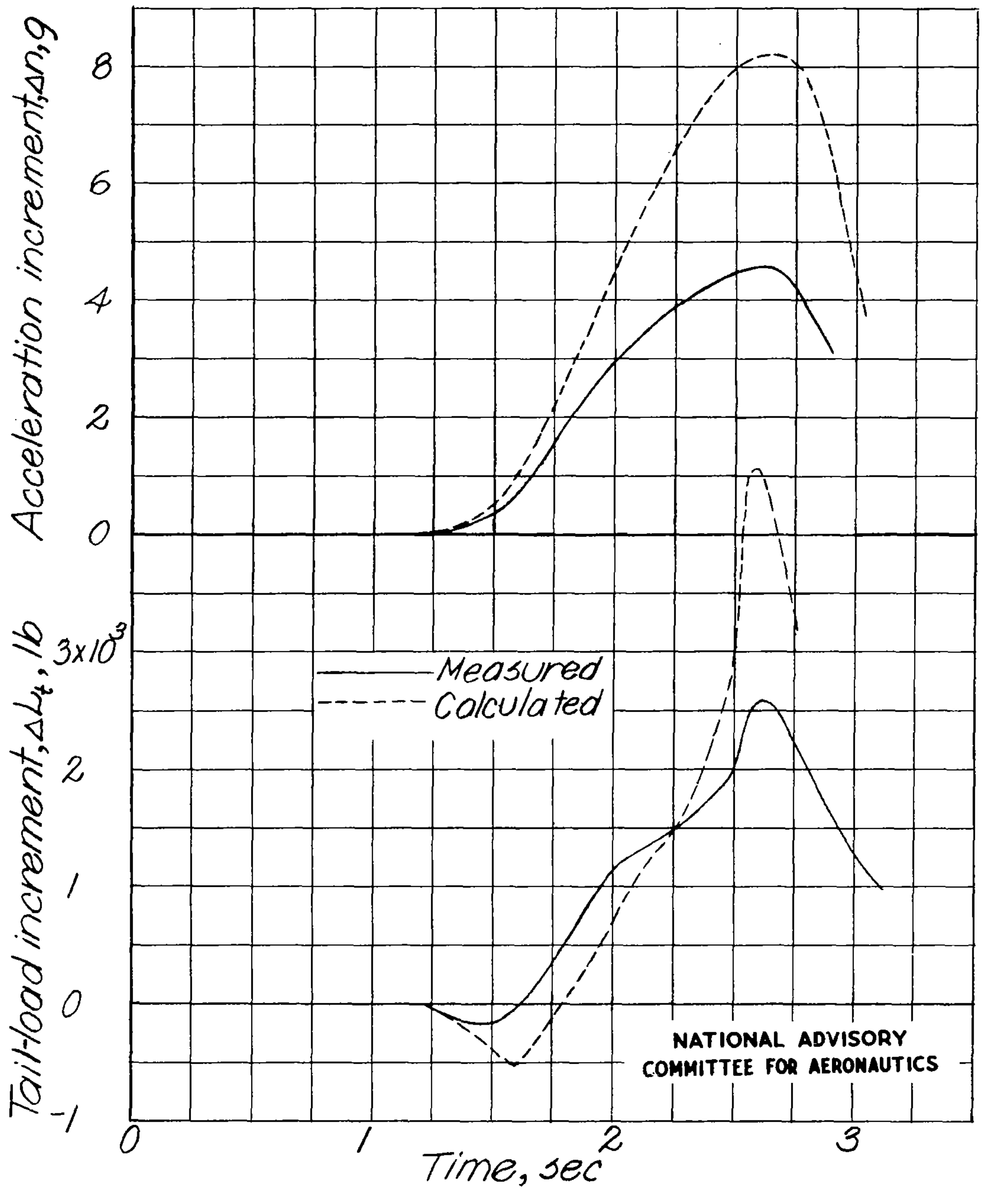

Figure 6.- Comparison between measured and calculated tail-load and acceleration increments during a dive pull-out in a P-40K airplane.

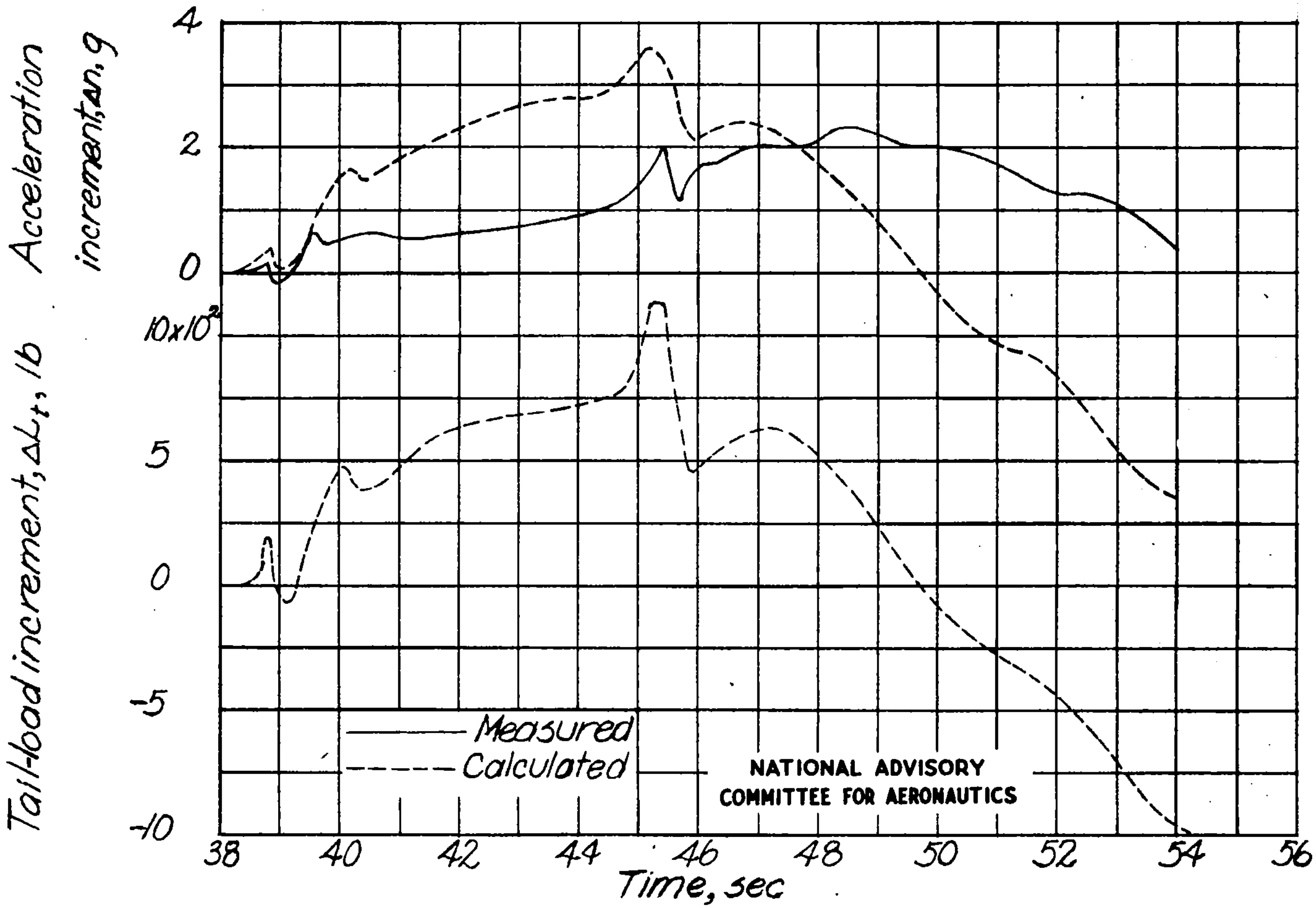

Figure 7.- Comparison between measured and calculated acceleration increments during a dive pull-out in an XP-51 airplane. Flight 26. (No tail load measured.)

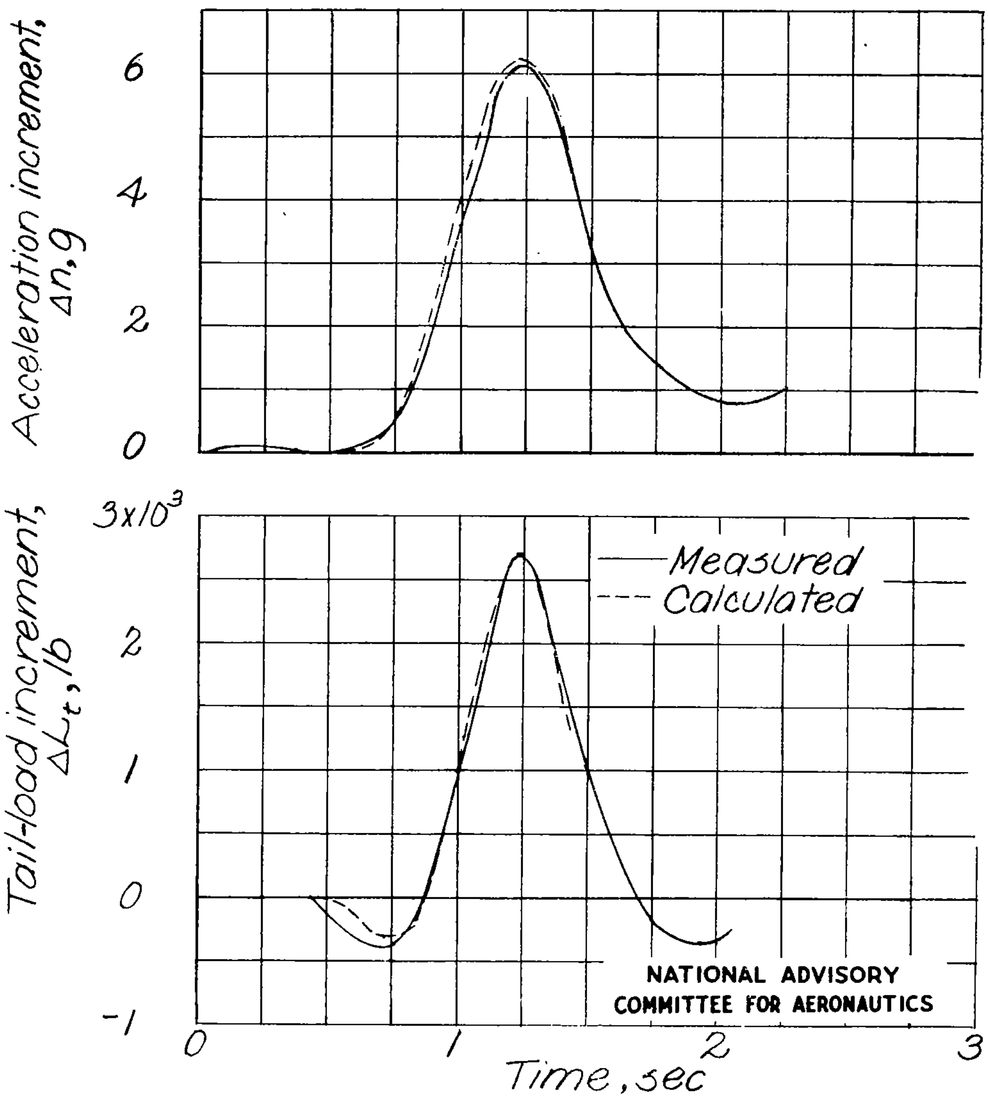

Figure 8.- Comparison between measured and calculated tail-load and acceleration increments during a dive pull-out in an XP-51 airplane. Flight 10.

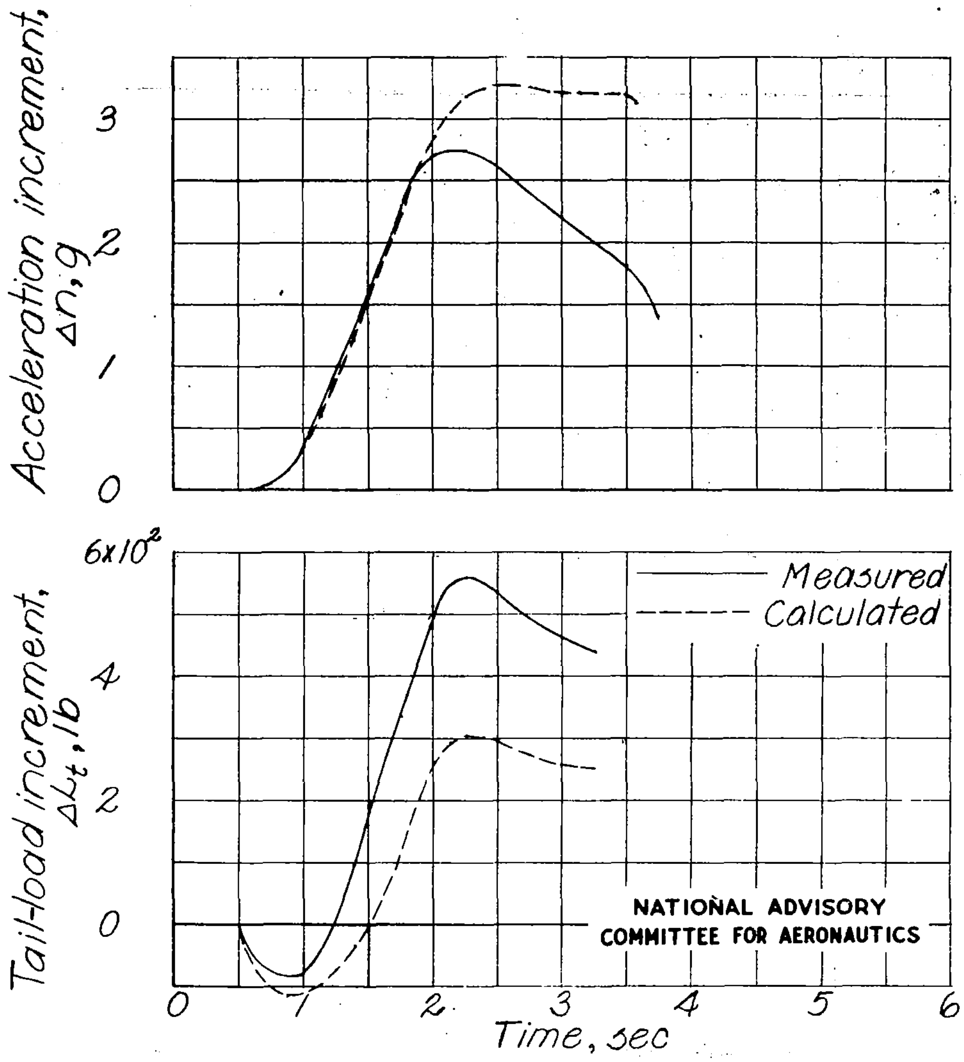

Figure 9.–Comparison between measured and calculated tail-load and acceleration increments during a pull-up in a BT-9B airplane.